Computer Physics Communications 180 (2009) 920–925

Contents lists available at ScienceDirect

Computer Physics Communications

www.elsevier.com/locate/cpc

Wavelet data analysis of EXAFS spectra

J. Timoshenko *, A. Kuzmin

Institute of Solid State Physics, University of Latvia, Kengaraga street 8, LV-1063 Riga, Latvia

ARTICLE INFO

Article history:
Received 5 August 2008
Received in revised form 21 November 2008
Accepted 12 December 2008
Available online 24 December 2008

PACS:
61.05.cj
78.70.Dm

Keywords:
X-ray absorption spectroscopy
Structure
Oxides
Wavelet analysis

ABSTRACT

The application of wavelet transform to the analysis of the extended X-ray absorption fine structure (EXAFS) from perovskite-type compounds is presented on the example of the Re L_3-edge in ReO_3 and Co K-edge in $LaCoO_3$. We propose a modified wavelet transform procedure, which allows better discrimination of the overlapped contributions into the EXAFS signal.

1. Introduction

Wavelet transform (WT) is a powerful method for the analysis of complex time-frequency signals [1], which has been widely used in different fields and applications such as sound and image processing, data compression and signal de-noising. Opposite to well-known Fourier transform (FT), the WT allows to obtain a two-dimensional representation of the periodic signal with simultaneous localization in time and frequency space domains. The use of WT for the analysis and interpretation of the extended X-ray absorption fine structure (EXAFS) spectra is continuously expanding during the last ten years [2–14]. It is believed that the WT can be useful for the EXAFS signal extraction, noise reduction, including the removal of the local deformations in the EXAFS signal as in de-glitching procedure, and a discrimination of atoms by their elemental nature in case of overlapping contributions.

The EXAFS signal extraction from the X-ray absorption coefficient based on the multi-resolution signal decomposition has been proposed in [2,5]. The approach uses the ability of WT to decompose a given signal into the high and low frequency parts, corresponding to the EXAFS signal and the background contribution, respectively. It has been successfully applied to the analysis of the Cu K-edge in copper [2,5] and the Si K-edge in a 6H a-SiC thin film [4].

The reconstruction of the radial distribution function from noisy EXAFS signals of copper has been performed in [3] based on the wavelet-Galerkin regularization method. In this method, the integral equation, describing the EXAFS signal, is discretized by projection onto discrete Daubechies-type wavelet subspaces and is solved by iterative procedure [3].

Another wide use of WT in the EXAFS data analysis is concerned with an identification of overlapping contributions, in particular, coming from neighboring atoms of different type or scattering events of different order such as single and multiple-scattering. This problem has been addressed through the use of a continuous Cauchy WT in [6,9–11] and the Morlet WT in [7,12,14]. Recently, the use of a combined FEFF-Morlet wavelet has been proposed [13], that improves a resolution of the wavelet ridges in energy and real space. The method takes into account the scattering properties of the atoms as computed within the FEFF formalism [15] and provides better discrimination of different atoms at similar distances than the Morlet wavelet [13].

In this work the application of WT to the different stages of the analysis, i.e. for visualization of atomic contributions and discrimination of different atoms, is described on the example of perovskite-type compounds ReO_3 [16] and $LaCoO_3$ [17]. The peculiarity of these compounds is that they contain both heavy and light elements, and distances between some of them are close, that complicates the application of traditional analysis methods. Finally, we propose a modified WT, which provides with a better localization of the EXAFS signal and, thus, allows better discrimination of the overlapped contributions.

* Corresponding author. Tel.: (+371) 67251691.
E-mail address: timoshenkojanis@inbox.lv (J. Timoshenko).

0010-4655/$ – see front matter
doi:10.1016/j.cpc.2008.12.020

2. Basic principles of EXAFS

The EXAFS signal $\chi(k)$ is an oscillating part of the X-ray absorption coefficient, arising from a scattering of the photoelectron, excited at the absorbing atom of particular type, by a potential of surrounding atoms. The frequency of the oscillations is proportional to the total scattering path length of the photoelectron, and thus, its analysis allows a discrimination of atoms groups, located at different distances around the absorber. An excellent review on the topic can be found in [18].

The total EXAFS signal can be described by a sum over infinite number of scattering events $\chi_j(k)$, called multiple-scattering (MS) contributions [18]

$$\chi(k) = \sum_j^{\infty} \chi_j(k), \tag{1}$$

where $\chi_j(k) = A(k)\sin(2kR + \Psi(k,R))$ is an oscillating function, depending on the scattering properties (amplitude $A(k)$ and phase $\Psi(k,R)$) of atoms involved into the scattering process and having the frequency given by the total scattering path length ($2R$). Note that an alternative decomposition of the total EXAFS signal can be performed over many-atom distributions [19].

A single-scattering curved-wave harmonic approximation is widely used to describe a contribution from a group of N atoms, located at close distance R from the absorber. In this case, the EXAFS signal can be written as [18]

$$\chi(k) = \frac{NS_0^2}{kR^2} e^{-2\sigma^2 k^2} e^{-2R/\lambda(k)} F(k,R) \sin\bigl(2kR + \Phi(k,R)\bigr), \tag{2}$$

where $k = \sqrt{(2m_e/\hbar^2)(E - E_0)}$ is the photoelectron wave number, m_e is the electron mass, $\hbar$ is the Plank's constant, E is the X-ray photon energy, E_0 is the binding energy of the photoelectron, S_0^2 is the scale factor taking into account amplitude damping due to the multielectron effects, σ is the mean square radial displacement or Debye–Waller factor, $\lambda(k)$ is the mean-free path of the photoelectron, $F(k,R)$ is the backscattering amplitude of the photoelectron and $\Phi(k,R)$ is the total phase shift, including the contributions of the central and backscattering atoms.

The easiest way to evaluate the interatomic distance R is to perform a spectral analysis using the FT [20]. However, if two groups of different atoms are located at close distances, their contributions in R-space overlap and become indistinguishable. For a compound, composed of light and heavy elements, as for example rhenium trioxide (ReO_3), one can note that heavy rhenium atoms have large values of the scattering amplitude $F(k,R)$ at higher values of wave numbers k, whereas light oxygen atoms – at low wave numbers. As a result, their contributions into the total EXAFS signal are differently localized in the k-space and, therefore, one can use this fact to discriminate them with the help of WT.

3. Conventional continuous wavelet transform

Wavelet transform of a given signal $\chi(k)$ is defined as

$$w(a,b) = \sqrt{a} \int_{-\infty}^{+\infty} \chi(k)\bar{\varphi}\bigl(a(k-b)\bigr)\,dk, \tag{3}$$

where $\varphi(k)$, called the "mother-wavelet", has non-zero value in a very short range of arguments. The bar over $\varphi(k)$ indicates that its complex conjugated function is used. For the so-called Morlet WT, the function $\varphi(k)$ is defined as

$$\varphi(k) = \exp(i\omega_0 k)\exp\bigl(-\sigma_0^2 k^2\bigr). \tag{4}$$

In further discussion, the parameter σ_0 equals always to 1 Å, since k is measured in $Å^{-1}$, and will be omitted. The meaning of parameter ω_0 will be given below. The mother-wavelet function $\varphi(k)$ differs from zero in a short range of argument values that makes a principle difference between WT and FT.

The more similar is the shape of the $\chi(k)$ signal and of the function $\varphi(k)$, the larger is the value of $w(a,b)$. By varying the values of parameters a and b, basic transformations of $\varphi(k)$, distortion and translation, are carried out, and the signal $\chi(k)$ is analyzed for a similarity with functions of different width in different ranges of argument values. Note that when high frequencies are present in the analyzed signal, the maximum of the function $w(a,b)$ is located at the large values of parameter a. Parameters of signal components k and ω are calculated using the relationships $b = k$ and $a = \omega/\omega_0$, which will be addressed below.

The resolution of the wavelet transform is limited by the width of wavelet function in k-space and ω-space, i.e. equals to $2\Delta_k$ and $2\Delta_\omega$. Since the wavelet transform is the integral of the product of wavelet function and signal, the value of $w(a,b)$ depends on the values of *all* signal points inside the interval $(b-\Delta_k; b+\Delta_k)$ and on the amplitudes of *all* signal frequencies in the range $(\omega a - \Delta_\omega; \omega a + \Delta_\omega)$. If there are such two contributions in the signal that the differences between their frequencies is smaller than $2\Delta_\omega$ or they are separated in k-space by distance smaller than $2\Delta_k$, they cannot be resolved. It can be written in the form of so-called uncertainty boxes as $[b \pm \Delta_k] \times [\omega_0 a \pm \Delta_\omega]$. Obviously the values of Δ_k and Δ_ω depend on the value of a. The general expressions of this dependency for any type of wavelet function can be easily obtained, here we will focus on the Morlet wavelet transform only. Let us estimate Δ_k as the second momentum of the square of wavelet function around its center, i.e. at the point $k = b$:

$$\Delta_k = \frac{1}{\|\varphi(k)\|}\sqrt{\int_{-\infty}^{+\infty}(k-b)^2 a \exp\bigl(-2a^2(k-b)^2\bigr)\,dk} = \frac{1}{2a}. \tag{5}$$

The Fourier transform of the Morlet wavelet function is

$$\begin{aligned}\hat{\varphi}(\omega) &= \int_{-\infty}^{+\infty} \exp\bigl(i\omega_0 a(k-b)\bigr)\exp\bigl(-a^2(k-b)^2\bigr)\exp(-i\omega k)\,dk \\ &= \sqrt{\frac{\pi}{a}}\exp\bigl(-(\omega_0 a - \omega)^2/\bigl(4a^2\bigr)\exp(-ib\omega)\bigr)\end{aligned} \tag{6}$$

and

$$\begin{aligned}\Delta_\omega &= \frac{1}{\|\hat{\varphi}(\omega)\|}\sqrt{\int_0^{+\infty}(\omega-\omega_0 a)^2\frac{\pi}{a}\exp\bigl(-(\omega_0 a-\omega)^2/\bigl(2a^2\bigr)\bigr)d\omega} \\ &= \frac{a}{2}.\end{aligned} \tag{7}$$

It can be seen now that

(1) the resolution in ω-space depends on the values of a, so it is different for different signal frequencies and results in a deformation of the signal image as will be described in details in the next section;
(2) the resolutions in ω-space and in k-space are inversely proportional, i.e. a good resolution in ω-space means poor resolution in k-space and vice versa;
(3) since $a = \omega/\omega_0$, the resolution can be easily changed by varying the value of the parameter ω_0.

The advantage of WT over FT can be illustrated (Figs. 1 and 2) on example of the two model signals $\chi_1(k)$ and $\chi_2(k)$

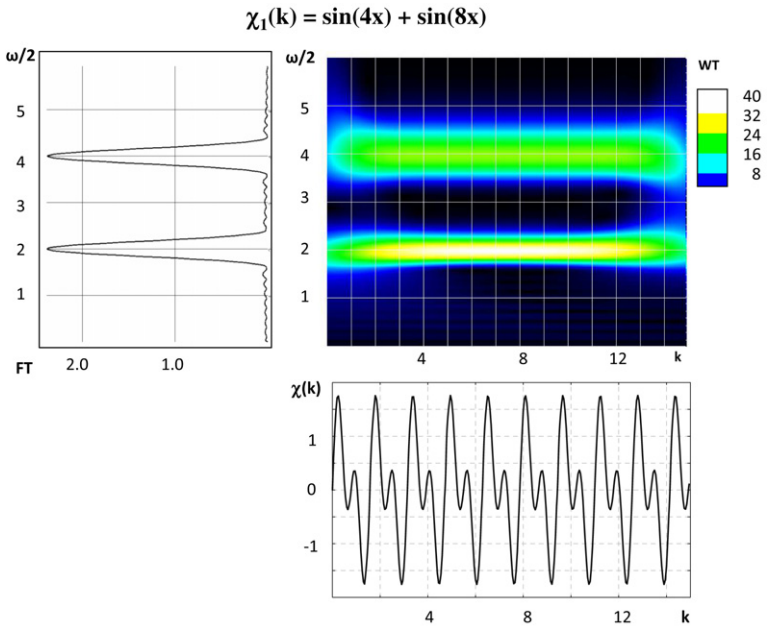

Fig. 1. (Color online) Model 1: initial signal $\chi_1(k)$ (bottom panel), modulus of its Fourier transform (left panel), modulus of its Morlet wavelet transform (central panel). See text for details.

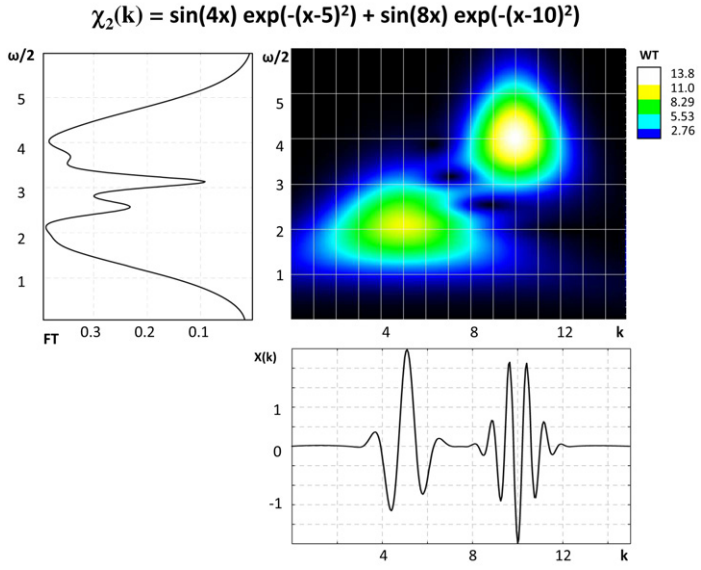

Fig. 2. (Color online) Model 2: initial signal $\chi_2(k)$ (bottom panel), modulus of its Fourier transform (left panel), modulus of its Morlet wavelet transform (central panel). See text for details.

$$\chi_1(k) = \sin(4k) + \sin(8k),$$
$$\chi_2(k) = \sin(4k)\exp\left(-(k-5)^2\right) + \sin(8k)\exp\left(-(k-10)^2\right). \quad (8)$$

The first signal $\chi_1(k)$ consists of a sum of two sinusoidal components, whereas the second one $\chi_2(k)$ is composed of two modulated by Gaussians sinusoidal signals, being well localized in two narrow k-ranges. Note that the shape of the $\chi_2(k)$ signal imitates the EXAFS from a system with two coordination shells, where the first shell consists of light atoms and the second shell – of heavy atoms.

The WT moduli for the two model signals are shown in Figs. 1 and 2 as a function of argument k and the frequency ω. Both methods (FT and WT) allow to observe the two components. However, the FT image, being a one-dimensional function, provides an information only on the components frequencies, whereas the WT allows additionally to evaluate their duration in the k-space.

One can see that the use of conventional Morlet WT for the second signal, constructed from the two components of equal duration in k-space, results in a two-dimensional function with two maxima, having different non-symmetric shapes. At the same time, its FT contains two symmetric maxima.

In Fig. 3 we show an example of the WT of the Re L_3-edge EXAFS spectra, taken from [16], in cubic perovskite-type polycrystalline ReO_3, which illustrates nicely the advantage of the WT over FT. The two maxima, located at different values of wave numbers and distances are observed in the WT. They correspond to the first two coordination shells around the rhenium atom, composed of six oxygen (the 1st shell) and six rhenium (the 2nd shell) atoms, respectively.

As it was mentioned before, due to the difference in the scattering amplitudes between heavy and light elements, the rhenium atoms produce stronger EXAFS signal at large values of the wave

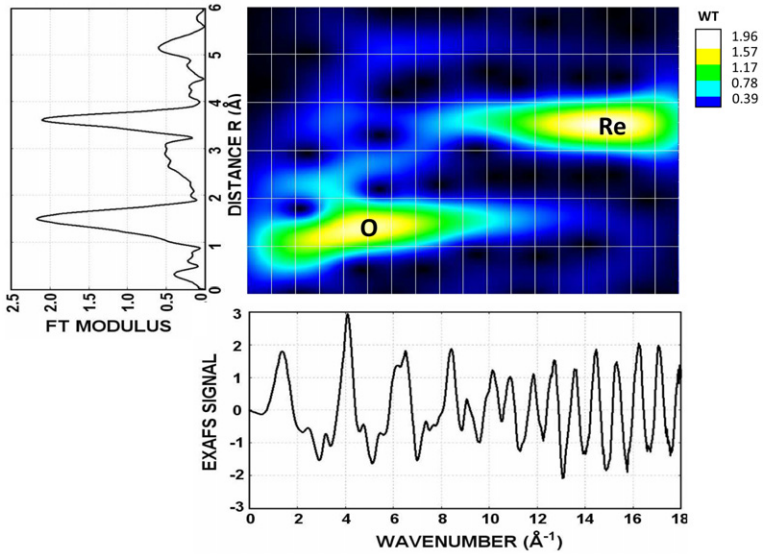

Fig. 3. (Color online) The Re L_3-edge EXAFS signal (bottom panel) in polycrystalline ReO_3 [16] at room temperature, its Fourier transform (left panel) and Morlet wavelet transform (central panel).

number k whereas the light oxygen atoms – at low k values, i.e. they are localized in different ranges of k-space. This fact is used in the WT to distinguish the two contributions. Note that conventional FT does not provide with such possibility. From Fig. 3, one can unambiguously conclude that the maximum at $R \sim 1.5$ Å, $k \sim 5$ Å^{-1} is due to the first oxygen shell, whereas the more distant maximum at $R \sim 3.5$ Å, $k \sim 15$ Å^{-1} is due to a group of rhenium atoms. Note that there are also visible some additional weak maxima corresponding to the multiple-scattering effects within the first coordination shell and to the distant coordination shells [21].

4. Modified wavelet transform

In this section we will introduce the modified wavelet transform, which allows to obtain a better localization of the EXAFS signal through the use of both high and low frequency parts of the EXAFS signal simultaneously.

First, let us consider the continuous Morlet WT of the signal, composed of three damped sinusoidal functions

$$\chi(k) = \sin(a_1 k)\exp\bigl(-(k-b_1)^2\bigr) + \sin(a_2 k)\exp\bigl(-(k-b_2)^2\bigr) + \sin(a_3 k)\exp\bigl(-(k-b_3)^2\bigr), \tag{9}$$

with $a_1 = 4$, $b_1 = 4$; $a_2 = 12$, $b_2 = 10$, $a_3 = 20$ and $b_3 = 16$. The signal is shown in Fig. 4 together with the modulus of its Fourier transform, which is composed of three maxima having close widths. Such signal is localized both in ω- and k-space.

The moduli of the continuous Morlet WT for different values of parameter ω_0 are shown in Fig. 5. Each plot has three pronounced maxima, but their shapes differ and depend on the value of the parameter ω_0. For frequencies much larger than ω_0, the maxima are stretched in the direction of the ω-axis, but for frequencies smaller than ω_0, the maxima are stretched in the direction of the k-axis. Such difference in the shapes complicates the interpretation of the obtained results. Besides, when ω_0 takes values far from the analyzed signal frequency, the maxima in conventional WT become broadened in the corresponding direction, and the information about their localization in ω or k-space gets lost. Note that the broadening effect is a general property of WT and is not specific for the Morlet transform only. More information on the properties of WT can be found in [22,23].

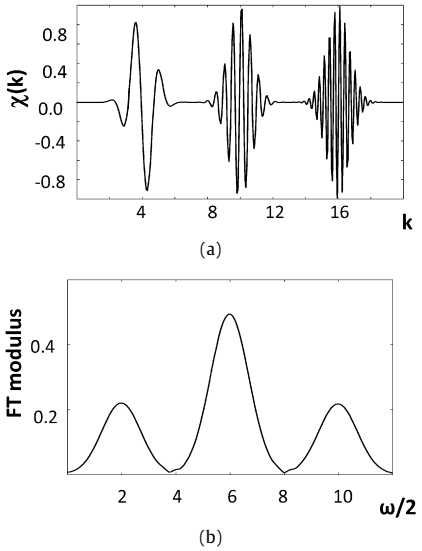

Fig. 4. Model signal (a) and its Fourier transform (b).

In order to find a solution for the described problem, we will examine the analytical expression of the continuous Morlet WT for harmonic signal, modulated by a Gaussian function

$$\chi(k) = \exp(i\omega_1 k)\exp\bigl(-\sigma^2 k^2\bigr). \tag{10}$$

By substituting Eq. (10) into Eq. (3) and performing integration, one obtains

$$w_{a,b} = \sqrt{\frac{\pi}{a}\gamma}\exp\bigl(-\gamma(\omega_0 a - \omega_1)^2/(2a)^2\bigr)\exp\bigl(-b^2\gamma\sigma^2\bigr) \times \exp(i\gamma\omega_1 b)\exp\bigl(i\omega_0 b\gamma\sigma^2/a\bigr), \tag{11}$$

where $\gamma = a^2/(a^2+\sigma^2)$, $0 \leqslant \gamma \leqslant 1$, and the modulus of the WT is

$$|w_{a,b}| = (w_{a,b}\overline{w_{a,b}})^{0.5} = (\pi\gamma/a)^{0.5}\exp\bigl(-\gamma(\omega_0 a - \omega_1)^2/(2a)^2\bigr)\exp\bigl(-b^2\sigma^2\gamma\bigr). \tag{12}$$

Here the first exponential term describes the localization of the transform result in the ω-space (and consequently the information

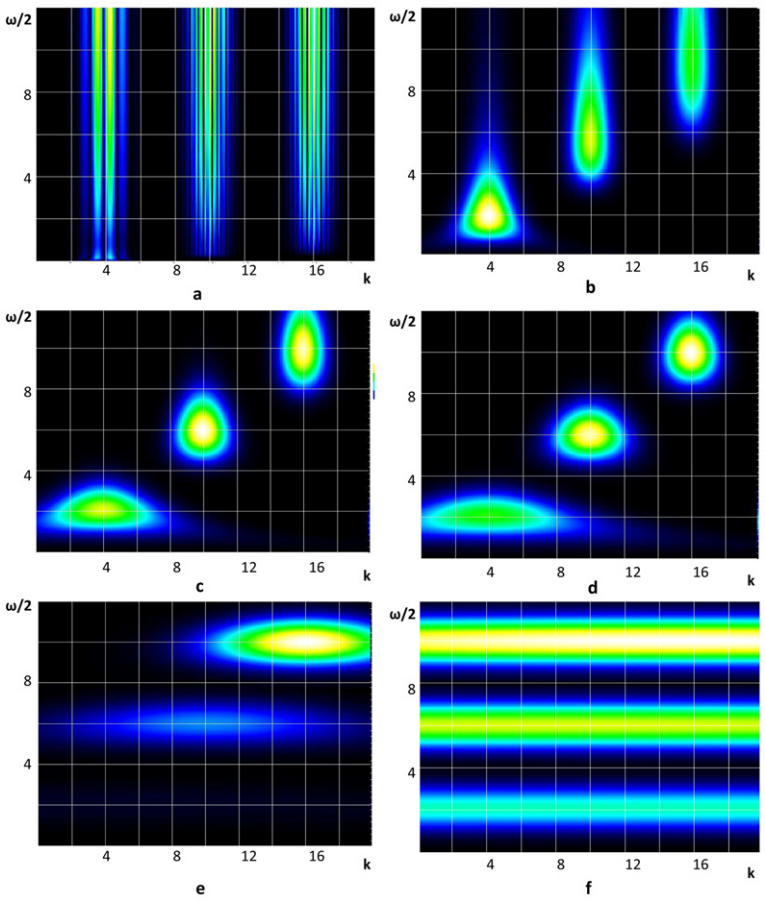

Fig. 5. (Color online) Moduli of the Morlet wavelet transform for the model signal $w_0 = 0.1$ (a), $w_0 = 4$ (b), $w_0 = 12$ (c), $w_0 = 20$ (d), $w_0 = 100$ (e), $w_0 = 1000$ (f).

about the localization in this space of initial signal), whereas the second exponential term acts in the k-space. For a signal of frequency ω_1 with a maximum at $k = 0$, the modulus of its Morlet WT reaches the maximum value for $b = 0$ and $a = \omega_1/\omega_0$.

Eq. (12) can be used to evaluate the deformations of the signal components images in a more quantitative way. The localization of the modulus of WT in the k-space is determined by the term $\exp(-b^2\sigma^2\gamma)$. Therefore, the width of the transform image along the k-axis (not to be confused with the width of the wavelet function, discussed above) can be described by the second moment of the square of this function (it can be associated with the energy of signal) around the zero point

$$\mu_b^2 = \int_{-\infty}^{+\infty} b^2 \exp\left(-2b^2\gamma\sigma^2\right) db = \frac{1}{4}\sqrt{\frac{\pi}{2\gamma^3\sigma^6}}. \tag{13}$$

Similarly, the exponential term $\exp(-\gamma(\omega - \omega_0 a)^2/(2a)^2)$ limits the image of WT in the ω-space, and one can estimate the width of the corresponding maximum along the ω-axis, using the approximation $a \approx \omega_1/\omega_0$, as

$$\mu_a^2 = \int_0^{+\infty} \left(a - \frac{\omega_1}{\omega_0}\right)^2 \exp\left(\frac{-\omega_0^2}{2(\frac{\omega_1}{\omega_0}^2 + \sigma^2)}\left(a - \frac{\omega_1}{\omega_0}\right)^2\right) da$$
$$= \frac{1}{2}\sqrt{2\pi\left((\omega_1/\omega_0)^2 + \sigma^2\right)^3/\omega_0^6}. \tag{14}$$

The deformation of the maximum can be defined as

$$\frac{\mu_b^2}{\mu_a^2} = \frac{1}{4}\left[\frac{\omega_0}{a\sigma}\right]^3. \tag{15}$$

Note that if $a \gg \omega_0$ ($\omega_1 \gg \omega_0$), then the image is distorted in the direction of ω-axis, and if $a \ll \omega_0$ ($\omega_1 \ll \omega_0$), then the distortion takes place in the direction of k-axis.

Based on Eq. (15), we propose the following modification of the WT: the value of parameter ω_0 is varied during the transformation, in order to keep the deformation of the image constant, independently on the frequency ω_1. This can be achieved if ω_0 varies proportionally to the value of the parameter a, i.e., $\omega_0 = ca$, where c is a positive constant, and the modified Morlet WT is given by

$$w(a,b) = \sqrt{a}\int_{-\infty}^{+\infty} \chi(k)\exp\left(-ica^2(k-b)\right)\exp\left(-a^2(k-b)^2\right) dk. \tag{16}$$

Note that unlike the conventional continuous Morlet transform, the mother-wavelet function in Eq. (16) changes for each value of a during the transformation. However, the transform, defined by Eq. (16), can also be considered as a set of many conventional continuous Morlet transforms, each carried in the range from $a - (da)/2$ to $a + (da)/2$. Therefore, the proposed transform inside of each of these intervals should have the same properties as a conventional continuous Morlet transform and, thus, can be called a wavelet transform. For instance, similarly to the conventional Morlet transform, also in the case of the proposed transform the resolution in k-space can be increased by reducing the resolution in ω-space (by decreasing the value of parameter c) and vice versa.

One should note again that the proposed transform does not provide a resolution better than the conventional wavelet transform, but assures that the resolution is the same for all values of a. This means also that the properties of proposed transform, related to its image in ω-space, differ from the properties of the conven-

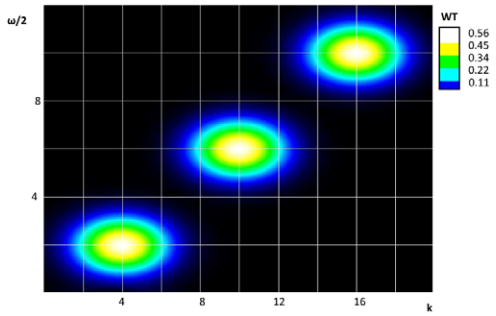

Fig. 6. (Color online) Modulus of the modified wavelet transform of the model signal. (To be compared with results in Fig. 5.)

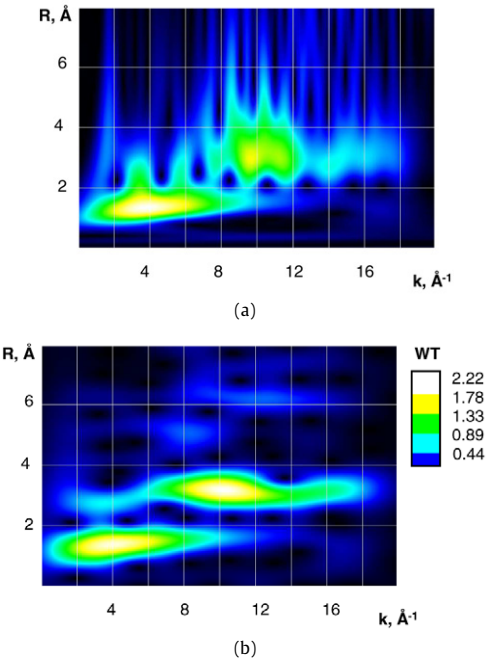

Fig. 7. (Color online) Modulus of the Morlet wavelet transform (a) and modulus of the modified wavelet transform (b) of the Co K-edge EXAFS signal in $LaCoO_3$.

tional wavelet transform. For instance, the equation for calculation of inverse wavelet transform, given in [22], cannot be directly applied to the modified transform.

The application of Eq. (16) to the model, given by Eq. (9), is illustrated in Fig. 6. The calculated image allows to obtain correct values of the frequencies of the signal components. Besides, the maxima, corresponding to the different components of the signal, do not overlap, are well localized and have similar shapes. Finally, the images of components with equal amplitudes have also equal magnitudes. Therefore, all this makes the visualization and interpretation of the results simpler.

Further we will discuss the use of the modified WT for the analysis of experimental EXAFS signals.

The conventional and modified WTs (Fig. 7) are applied to the Co K-edge EXAFS signal in $LaCoO_3$, taken from [17]. One can see, that the most noticeable maxima, corresponding to the oxygen at $R \sim 1.5$ Å, $k \sim 4$ Å^{-1} and cobalt at $R \sim 3.5$ Å, $k \sim 10$ Å^{-1} atoms, have significantly better localization in the case of the modified WT. Also the maxima, corresponding to more distant atoms and multiple-scattering effects (the peaks at 5 and 6 Å), are distorted and cannot be discriminated in the case of Morlet WT, but they are well enough localized in the modified WT image that makes their separation possible.

5. Conclusions

The application of wavelet transform to the analysis of the EXAFS signals of perovskite-type compounds is demonstrated on the example of ReO_3 and $LaCoO_3$. We found that the wavelet transform is advantageous method compared with conventional Fourier transform both for visualization and interpretation of the EXAFS spectra, especially, for compounds composed of heavy and light elements.

The modified wavelet transform is proposed, which gives better localization, allowing to operate with high and low frequency parts of the EXAFS signal simultaneously, and, thus, provides easier interpretation of results.

To conclude, the wavelet transform is a powerful and flexible method which can replace the Fourier transform in all its applications to the EXAFS data analysis, providing even more information and allowing more detailed studies.

Acknowledgements

This work was partially supported by the Latvian Research Grant 05.1717.

References

[1] Q. Tao, V.I. Mang, X. Yuesheng (Eds.), Wavelet Analysis and Applications, Birkhäuser-Verlag, Basel, 2007.
[2] X. Shao, L. Shao, G. Zhao, Anal. Commun. 35 (1998) 135.
[3] K. Yamaguchi, Y. Ito, T. Mukoyama, M. Takahashi, S. Emura, J. Phys. B 32 (1999) 1393.
[4] S. Muto, J. Electron. Microscopy 49 (2000) 525.
[5] L. Shao, X. Lin, X. Shao, Appl. Spectroscopy Rev. 37 (2002) 429.
[6] M. Muñoz, P. Argoul, F. Farges, Am. Mineral. 88 (2003) 694.
[7] H. Funke, A.C. Scheinost, M. Chukalina, Phys. Rev. B 71 (2005) 094110.
[8] G.E. Brown, J.G. Catalano, A.S. Templeton, T.P. Trainor, F. Farges, B.C. Bostick, T. Kendelewicz, C.S. Doyle, A.M. Spormann, K. Revill, G. Morin, F. Juillot, G. Calas, Phys. Scripta T 115 (2005) 80.
[9] M.M. Muñoz, F. Farges, P. Argoul, Phys. Scripta T 115 (2005) 221.
[10] H. Funke, M. Chukalina, A. Rossberg, Phys. Scripta T 115 (2005) 232.
[11] M. Harfouche, E. Wieland, R. Dahna, T. Fujita, J. Tits, D. Kunz, M. Tsukamoto, J. Colloid Interface Sci. 303 (2006) 195.
[12] M. Vespa, R.D. Daehn, D. Grolimund, E. Wieland, A.M. Scheidegger, Environ. Sci. Technol. 40 (2006) 2275.
[13] H. Funke, M. Chukalina, A.C. Scheinost, J. Synchrotron. Rad. 14 (2007) 426.
[14] M. Sahnoun, C. Daul, O. Haas, J. Appl. Phys. 101 (2007) 014911.
[15] A.L. Ankudinov, B. Ravel, J.J. Rehr, S.D. Conradson, Phys. Rev. B 58 (1998) 7565.
[16] J. Purans, G. Dalba, P. Fornasini, A. Kuzmin, S. De Panfilis, F. Rocca, AIP Conf. Proc. 882 (2007) 422.
[17] V. Efimov, E. Efimova, D. Karpinskii, D.I. Kochubey, V. Kriventsov, A. Kuzmin, S. Molodtsov, V. Sikolenko, S. Tiutiunnikov, I.O. Troyanchuk, A.N. Shmakov, D. Vyalikh, Phys. Stat. Solidi (c) 4 (2007) 805.
[18] J.J. Rehr, R.C. Albers, Rev. Mod. Phys. 72 (2000) 621.
[19] A. Filipponi, A. Di Cicco, C.R. Natoli, Phys. Rev. B 52 (1995) 15122.
[20] D.E. Sayers, E.A. Stern, F.W. Lytle, Phys. Rev. Lett. 27 (1971) 1204.
[21] A. Kuzmin, J. Purans, M. Benfatto, C.R. Natoli, Phys. Rev. B 47 (1993) 2480.
[22] C.K. Chui, An Introduction to Wavelets, Academic Press, San Diego, 1992.
[23] S. Mallat, A Wavelet Tour of Signal Processing, Academic Press, San Diego, 1999.